ISSN: 0369-8963

Numerical Analysis of Fluid Dynamics and Heat Transfer from Flow Over Square Cylinder Using Ag-Water Nanofluid

ARUN SENTHIL KUMAR ATHINARAYANAN[1*], MANIKANDAN GURUNATHAN[2] AND RAJESH KANNA PARTHASARATHY[3]

[1, 2] Department of Mechanical Engineering, Velammal College of Engineering and Technology, Madurai, Tamilnadu, India.

[3]Department of Mechanical Engineering, Al Ghurair University, Dubai, United Arab Emirates.

Corresponding author: ARUN SENTHIL KUMAR ATHINARAYANAN

2D laminar flow over a square cylinder was numerically studied in an adiabatic channel to find the effect of nanofluids on heat transfer and fluid dynamics. The stream function vorticity formulation is employed to solve the present situation. In the laminar range, the effect of the volume fraction of the nanoparticles was investigated for various Reynolds numbers. Heat transfer and fluid dynamics reports were documented in detail for steady-state conditions. Reattachment lengths, streamline contours, isothermal contours, local Nusselt numbers, and average Nusselt numbers were reported for the blockage ratio of 0.25. The symmetrical vortices sizes are increasing with the increase in the Reynolds number and volume fraction. The Reynolds number is more pronounced for the variation in the drag coefficient and the lift coefficient is majorly dependent on volume fraction.

Keywords: *heat transfer, nanofluid, laminar flow, re-circulation, square cylinder*

Introduction

Large industrial and consumer applications focus the attention on the flow over the bluff body in recent times for its complex fluid dynamics and accessibility to the physics behind it. Okajima [1] investigated the laminar flow over a square cylinder to correlate the vortex shedding, lift and drag coefficients and frequency of vortex shedding. The effect of blockage ratio of a square cylinder placed in a channel was numerically investigated using Strouhal number and Reynolds number by Mukhopadhyay *et al.*, [2]. In a confined environment, the blockage ratio dominates the vortex shedding of the flow over a square block. The value of the Strouhal number increases with the increase in the blockage. They also observed that an increment in the Reynolds number shows a minimal change in the Strouhal number. Several studies were conducted on bluff bodies with polygonal shapes to discover the effects of incident angle [3-5]. Sharma and Eswaran, [6] analyzed the flow and heat transfer from a square cylinder and presented the results for a free stream with a blockage ratio of 0.05. The vortex shedding starting at when the Reynolds number becomes Re > 50. They found that increasing Reynolds number results in an asymptotical increase in the Strouhal number. They also found that the top

 https://doi.org/10.37896/pd91.3/91342

ISSN: 0369-8963

wall and bottom wall average Nusselt numbers of the cylinder were the same and the front face of the square cylinder always gets the highest value than other walls.

In the recent trends, the field of heat transfer augmentation giving more attention to the usage of nanofluids due to their inherent properties and characteristics such as without notable pressure drops it can increase the heat transfer rates. Many researchers have investigated the significance of nanofluids on heat transfer [7-10]. They proved that the nanofluids are showing a notable improvement in heat transfer applications. By considering that, the flow separation region was studied which has the lower heat transfer than other regions and such work was done by Abu-Nada [11]. The author investigated the backward facing step (BFS) flow for convective heat transfer using different nanofluids. The results show that the higher thermal conductivity of the nanofluid increased in all the regions around the cylinder except recirculation zones. In a similar study Al-aswadi *et al.*, [12] analyzed the effects of flow over backward facing step using various nanofluids. In a similar study, Mohammed *et al.*, [13] studied the convective heat transfer from BFS. They found that the nanofluids produced a higher Nusselt number within the first recirculation zone. They also found that the SiO_2 nanoparticles which have lower thermal conductivity produce the higher Nusselt number at the recirculation zones in downstream. There are many experimentations were done on circular pipe flow using nanofluids [14], [15]. The heated parallel plates were studied numerically using Cu based nanofluid in the laminar range by Apurba *et al.,* [16]. They tested heat transfer by considering the fluid models as both Newtonian and non-Newtonian. Prasenjit and Das [17] found that the nanoparticles in the fluid increased the heat transmission rate of the fluid and make a major difference when compared with base fluid. Recently, Hojjat [18] highlighted the effects of nanoparticles in the base fluid and analyzed the effects of varying the aspect ratios of the rectangular ducts. The inclination effects of the heat transfer were discussed by Derouich *et al.,* [19] using an oscillating square cylinder. They computed the results for lower Reynolds numbers in the range of 40 to 220. They observed the change in the heat transfer rate by varying the parameters such as Reynolds number, frequency, amplitude and blockage ratio.

Numerous investigations were carried out to record the effect of confinement, effect angle of incidence, effect of splitter plate, force and mixed convection heat transfer, tandem square cylinder setup. Still, there are some gaps to be filled up in the study of flow over the square cylinder with the application of nanofluids. In the recent times the nanofluids are used in many real-time applications and creates a need for the current study. The present work discusses the effects nanofluids in fluid dynamics and heat transfer.

Mathematical formulation and numerical procedure

The schematic of the problem is depicted in the figure. 1. For the present study, incompressible two-dimensional laminar flow is considered. The Navier-Stokes equations in the primitive variable form [11][12] were considered as governing equations and solved by the stream-function vorticity formulation. The main objective of this study is to find the augmentation of heat transfer using Ag based nanofluid.

 https://doi.org/10.37896/pd91.3/91342

ISSN: 0369-8963

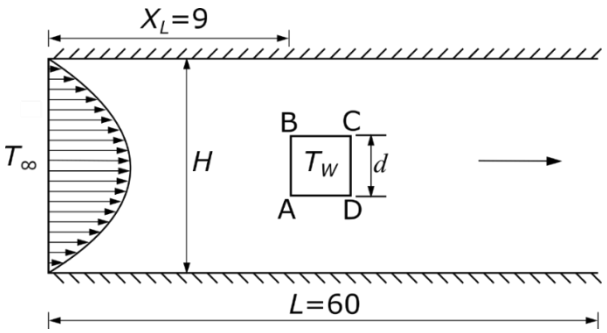

Figure 1. Schematic of flow with boundary conditions

Governing equations: (in non-dimensional form)

– In the below equations, ψ is stream function and u $= \partial\psi/\partial y$, v $= -\partial\psi/\partial y$, $\omega = (\partial \mathrm{v}/\partial x) - (\partial u/\partial y)$

– Stream function equation

$$\nabla^2\psi = -\omega \tag{1}$$

– Vorticity equation

$$\frac{\partial\omega}{\partial t} + \frac{\partial(u\omega)}{\partial x} + \frac{\partial(v\omega)}{\partial y} = \frac{1}{Re(1-\phi)^{2.5}\left[(1-\phi) + \phi\frac{\rho_s}{\rho_f}\right]}\nabla^2\omega \tag{2}$$

– Energy equation

$$\frac{\partial\theta}{\partial t} + \frac{\partial(u\theta)}{\partial x} + \frac{\partial(v\theta)}{\partial y} = \frac{\left(\frac{k_{nf}}{k_f}\right)}{Re\,Pr\left[(1-\phi) + \phi\frac{(\rho C_p)_s}{(\rho C_p)_f}\right]}\nabla^2\theta \tag{3}$$

The variables are scaled as, $u = \bar{u}/\bar{u}_0$, v$= \bar{v}/\bar{u}_0$, $x = \bar{x}/H$, $y = \bar{y}/H$, $t = \bar{t}/(H/\bar{u}_0)$. The dimensional variables indicated with overbars. Where, ϕ – volume fraction of nanoparticles, ρ_s – particle density, ρ_f – fluid density, Re – Reynolds number and Re $= \bar{u}_0 H/\nu$. Here, $\bar{u}_0$ – average horizontal velocity of the fluid, H – Channel height in the downstream, ν – kinematic viscosity of the fluid. According to Brinkman [20], the particles in the nanofluid suspension are considered as fine spherical particles and the viscosity of the fluid ρ_f was combinedly used. The effective viscosity of the nanofluid was used to simulate the Backward Step Flow problem by Al-Aswadi et al., [12]. The same nanofluid model was used to simulate the step flow by Abu-Nada [11]. The expression for effective viscosity is,

$$\mu_{nf} = \frac{\mu_f}{(1-\phi)^{2.5}} \tag{4}$$

The above eq. (4) is simulated for a two-sided lid-driven cavity with nanofluid by Tiwari and Das [21].

According to that the effective density,

 https://doi.org/10.37896/pd91.3/91342

ISSN: 0369-8963

$$\rho_{nf} = (1-\phi)\rho_f + \phi\rho_s \quad (5)$$

Khanafer et al., [22] used the following eq. (6) to find the heat capacity of nanofluid,

$$(\rho C_p)_{nf} = (1-\phi)(\rho C_p)_f + \phi(\rho C_p)_s \quad (6)$$

Maxwell-Garnetts (MG model) approximation of spherical nanoparticle is used to calculate the effective thermal conductivity. Tiwari and das [21] and Muthamilselvan et al., [23] used the MG model nanoparticles and investigated the mixed convection for cavity flow. The forced convection from step flow was analyzed by Abu-Nada [11] used this model for the laminar range. Christopher et al., [24] used the MG model for sudden expansion flow. In the prior work of the authors [25] the same model was successfully tested and also used in the current investigation:

$$\frac{k_{nf}}{k_f} = \frac{k_s + 2k_f - 2\phi(k_f - k_s)}{k_s + 2k_f + \phi(k_f - k_s)} \quad (7)$$

The channel blockage ratio is taken as 0.25 for the current investigation. As the part of boundary conditions the parabolic profile is considered at the inlet in the horizontal direction and the average velocity of the flow is,

$$\frac{\partial^2\psi}{\partial x^2} = 0\,, \quad \frac{\partial\omega}{\partial x} = 0\,, \frac{\partial u}{\partial x} = 0, \quad \frac{\partial\theta}{\partial x} = 0 \quad (8)$$

At solid boundaries:

$$u = 0\,, \quad v = 0 \quad (9)$$

Convergence of vorticity eq (2):

$$\varepsilon = \Sigma_{i,j=1}^{imax,jmax}(\omega_{i,j}^{n+1} - \omega_{i,j}^{n}) \quad (10)$$

Convergence of temperature eq (3):

$$\varepsilon = \Sigma_{i,j=1}^{imax,jmax}(\theta_{i,j}^{n+1} - \theta_{i,j}^{n}) \quad (11)$$

Rectangular grids are used to discretize the governing equations. The convective and diffusive terms are solved using central differencing scheme [26]. Gauss-Seidal method is used to solve the stream function eq. (1). Alternate Direction Implicit (ADI) scheme is used to solve the (2) and (3) along with eq. (1) until the arrival of a steady-state solution. The numerical procedures are referred from Das M K and Kanna P R [27]. The vorticity eq. (10) is discretized and monitored for every time step until the residue becomes less than 0.00001. As time marches in the calculation u and v velocities are monitored for the subsequent time steps and the steady is achieved when the differences are negligibly small. Furthermore, the summation of $(u^2+v^2)/2$ is checked for all discreet nodes with steady-state condition. This shows the steady-state is attained with total kinetic energy. Eq. (3) gives the steady-state heat transfer results. Heat transfer results are monitored by eq. (11).

Code validation and grid independence study

The author [25] has used the same code and boundary conditions to solve similar cases with Cu-water nanoparticles. Due to brevity, the validation has been shortened with the following description. The numerical simulation was conducted with and without nanoparticles

 https://doi.org/10.37896/pd91.3/91342

ISSN: 0369-8963

to validate the code. In a channel the flow over a square cylinder was simulated the blockage ratio, 0.125 [28] by considering air as working fluid. The initial creep flow was commenced for Re = 1. For Re = 30 the flow was separated as two stable vortexes were generated at the rear side wall of the square block. When compared with Breuer et al., [28] the current paper has a coarser grid which causes a discrepancy in the reattachment length. The author used 96,000 grid volumes in contrast the present study has a 15% percentage of it. For Re=60 and 200, the instantaneous streamlines were compared. Flow propagates in downstream which was separated from the bottom wall at higher Reynolds number. With a nonlinear trend the Reynolds and Strouhal numbers are increasing proportionately to a local maximum and after, the trend becomes down.

Grid independence study was conducted with non-uniform grids and the minimum grid space attained is 0.03. The study was carried out for Ag-based nanofluid for time marching with time step 0.001 was maintained to get the steady-state results with Re = 40 and ϕ = 0.1.

Table 1. Grid independence study; Ag nanoparticles Re = 40 and ϕ = 0.1

Grids	X_{r1}	Cylinder average Nusselt number
151 ×91	1.864	11.43
181 ×91	1.881	11.82
221 ×101	1.923	12.64
291 ×121	1.952	13.52
321 ×151	1.959	13.55

Results and discussion

It is found that the heat transfer is influenced by Reynolds number and volume fraction. The results were recorded for streamline contours, friction coefficient, isothermal contours, average and local Nusselt numbers. The mean and default values were set as ϕ = 0.03, Re = 30 and Ag nanoparticles were chosen. The Prandtl number of 6.2 is taken for pure water. Reynolds number and volume fractions are varied to find the effect of nanoparticles in the base fluid in the flow over a square cylinder. The volume fraction is varied from $0.0 \leq 0.1$ and the Reynolds number is varied from 10 to 40. Adiabatic conditions are assumed at the channel walls and the entry of the nanofluid is with the ambient condition, θ = 0.0. The local Nusselt number is evaluated from the below equation,

$$Nu = -\frac{k_{nf}}{k_f}\frac{\partial\theta}{\partial y}\bigg|_w \tag{12}$$

Average Nusselt number is measured from,

$$\overline{Nu} = -\frac{1}{L}Nu(x)\,dx \tag{13}$$

Fluid dynamics

In a confined channel, the flow over a single square cylinder was simulated with the steady-state condition. Various Reynolds number and volume fractions were compared by using streamline contours in fig 2. The base fluids are used to find the effects of nanoparticles

 https://doi.org/10.37896/pd91.3/91342

ISSN: 0369-8963

in nanofluids. At the front face of the cylinder the upstream fluid flow gets stagnated and in the downstream the it starts to bifurcated. At the symmetrical plane, the separated flow is reattached and forms the matching pairs of vortices. Further, the vortices are recorded for the range of Reynolds numbers varying from 20 to 40 in fig 2. When the Reynolds number increased the reattachment length is increased in the linear direction. The flow gets separated only at the rear face and not at the bottom or top walls. The nanoparticles are introduced in the base fluid as ϕ = 0.03 to reveal their role of it. Role of volume fraction can be found using eq. (2). The reattachment length (X_r) is varied for the same Reynolds number and for the change in ϕ (e.g., for Re = 20: ϕ = 0.0, X_r = 0.67; ϕ = 0.03, X_r = 0.96, i. e. 43.3% rise in X_r). Till Re = 40 the increase in such percentage continues (for Re = 40: ϕ = 0.0, X_r = 1.34; ϕ = 0.03, X_r = 1.83, i.e., 36.6% rise in X_r). The change in the inertia force occurs after the introduction of nanoparticles to the base fluid causes the increasing trend and it shows the significance of nanoparticles. Further by fixing Re = 30, volume fractions were varied as ϕ = 0.06 and ϕ = 0.1. Streamline contour for Re = 30 and ϕ = 0.06 is shown in fig. It is observed that when volume percentage ϕ increases to 0.06 from 0.03, the reattachment length Xr increased to 1.299 from 1.235 and it is increased further to 1.487 for ϕ = 0.1 diagram 2(h). It is noticed that when ϕ value increased the recirculation bubble size is also get increased. However, the Reynolds number is more pronounced than the ϕ value in flow separation.

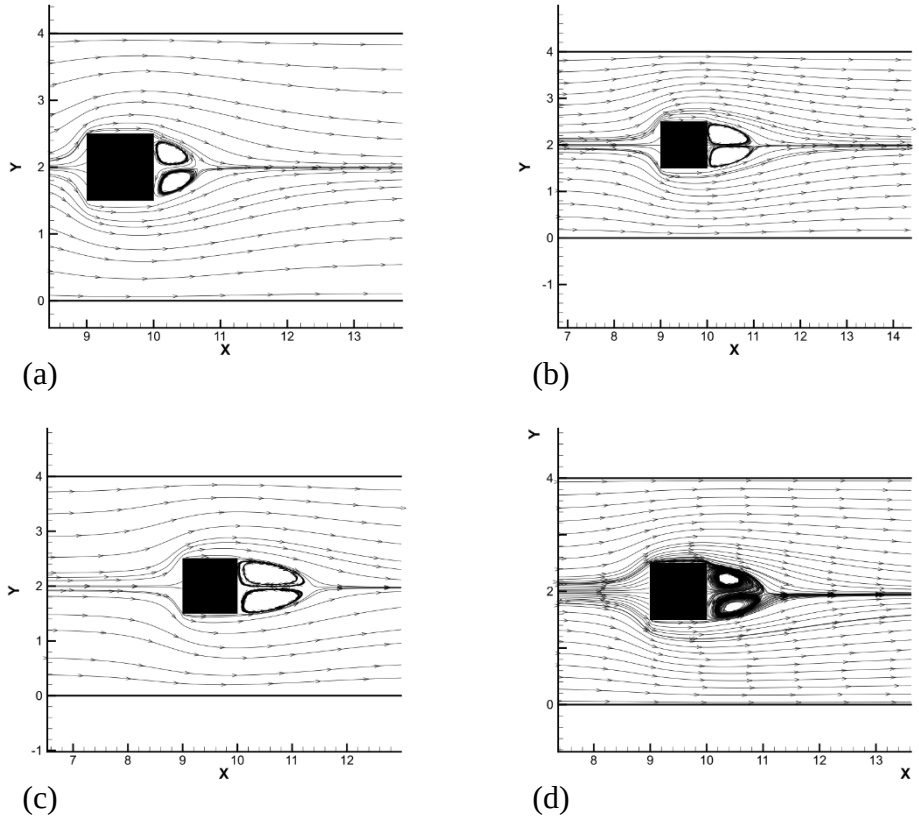

 https://doi.org/10.37896/pd91.3/91342

ISSN: 0369-8963

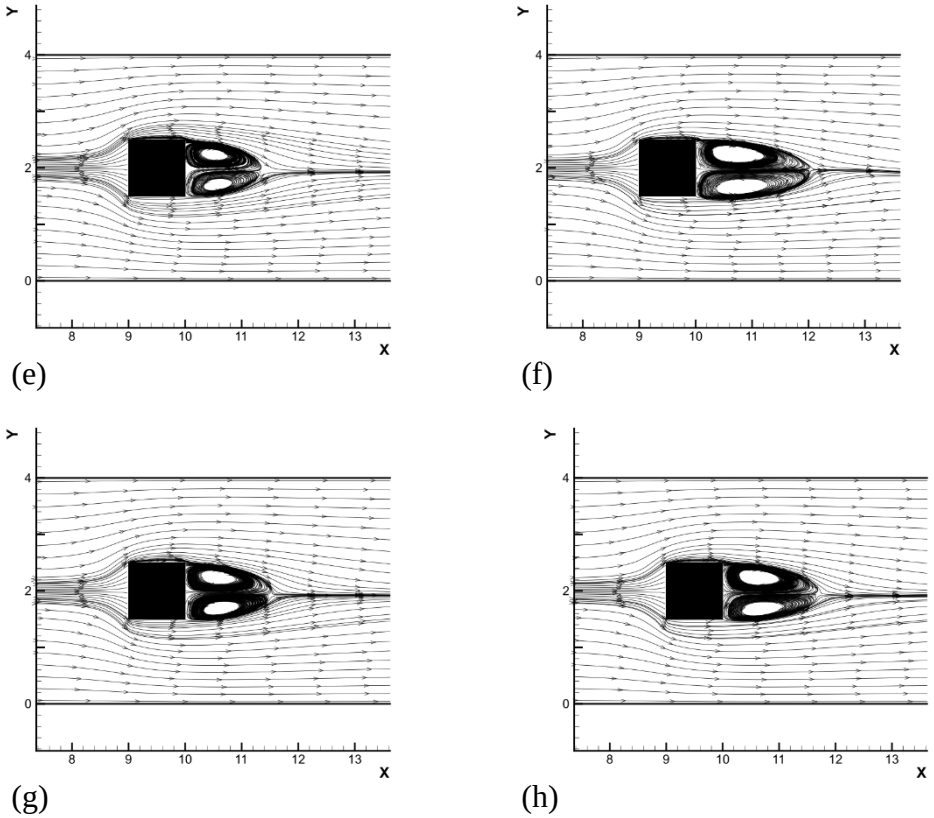

Figure 2. Streamline contour: effect of Reynolds number and ϕ; for ϕ = 0.0: (a) Re = 20, (b) Re = 30 (c) Re = 40; for ϕ = 0.03: (d) Re = 20, (e) Re = 30, (f) Re = 40; (g) ϕ = 0.06, Re = 30; (h) ϕ = 0.10, Re = 30

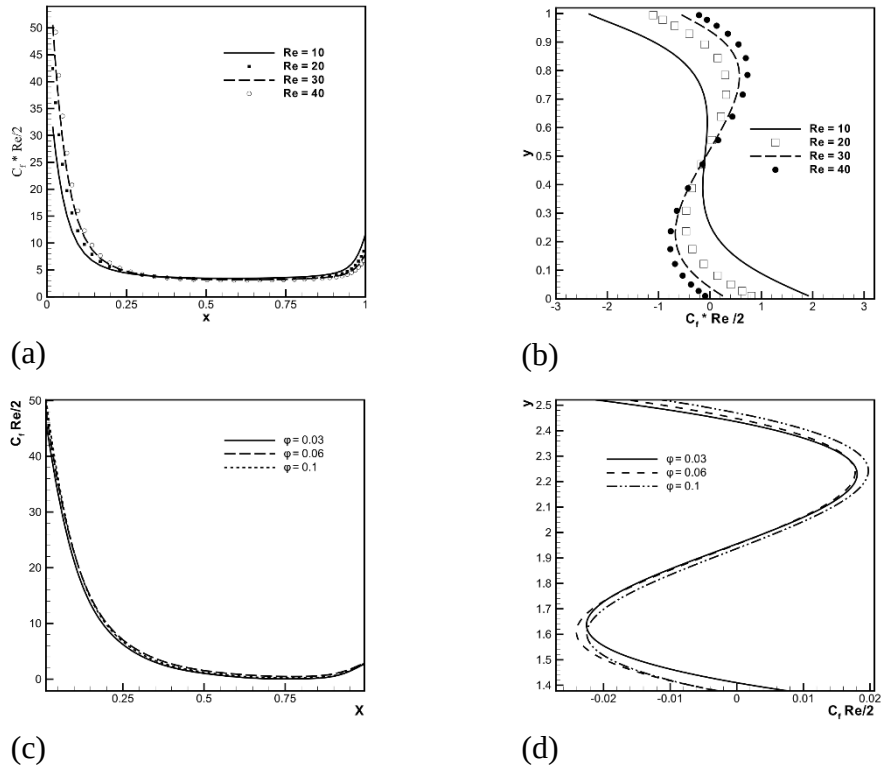

 https://doi.org/10.37896/pd91.3/91342

ISSN: 0369-8963

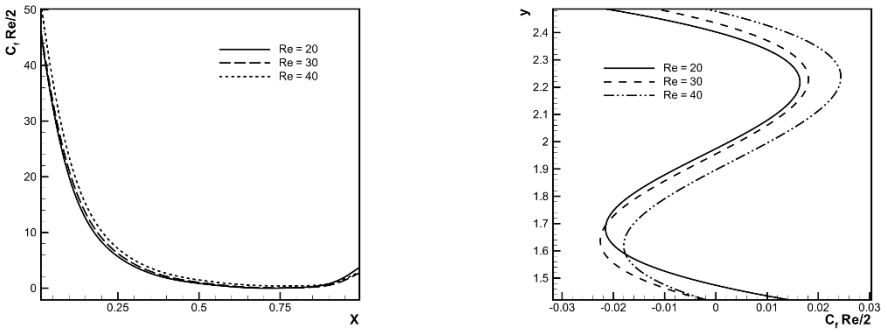

(e) (f)

Figure 3. Friction coefficient: Effect of Reynolds number and ϕ; (a) lift coefficient ϕ = 0.0, (b) drag coefficient ϕ = 0.0, (c) lift coefficient Re = 30, (d) drag coefficient Re = 30, (e) lift coefficient ϕ = 0.03, (f) drag

Fig. 3 depicts the friction coefficient. Initially, the base fluid without nanoparticles is tested and noticed that the friction coefficient at the cylinder corners is larger. Further, it reduced along the walls of the cylinder and again gets higher near the end of the walls fig 3(a). Other than the corners the coefficient of friction is less sensitive to the Reynolds number. Although, the Reynolds number is more pronounced for drag coefficient fig. 3(b). The rotating vortices with clockwise and counter-clockwise rotations are attached to the rear cylinder of the wall. The friction coefficient results produce a nonlinear tendency at the rear wall. The friction coefficient value of the base fluid increases with an increase in the Reynolds number and beyond a critical value, the trend is less sensitive to it. The friction coefficient is decreased significantly after the introduction of nanoparticles to the base fluid fig 3(e). The same trend follows for the increment in Reynolds number with constant volume fraction ϕ.

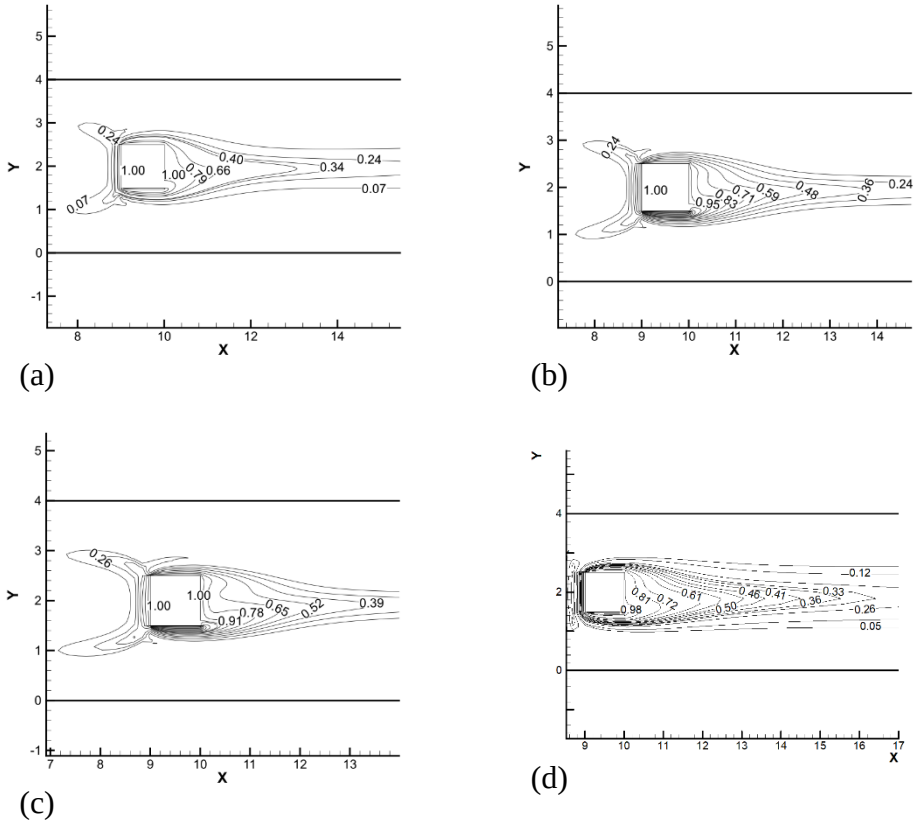

(a) (b)

(c) (d)

https://doi.org/10.37896/pd91.3/91342

ISSN: 0369-8963

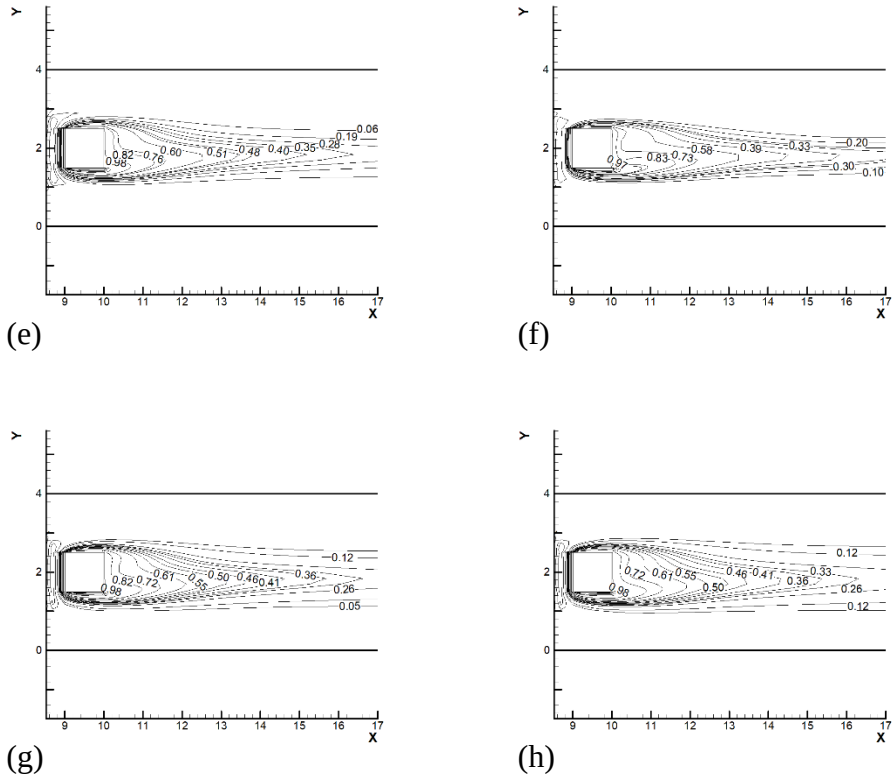

Figure 4. Streamline contour: effect of Reynolds number and ϕ; (a) Re = 20, ϕ = 0.0, (b) Re = 30, ϕ = 0.0, (c) Re = 40, ϕ = 0.0, (d) Re = 20, ϕ = 0.03, (e) Re = 30, ϕ = 0.03, (f) Re = 40, ϕ = 0.03, (g) Re = 30, ϕ = 0.06, (h) Re = 30, ϕ = 0.10

Heat Transfer

The wall temperature of the cylinder is maintained constantly. Hence the temperature is considered as non-dimensional, the temperature inside the cylinder q =1 and ambient temperature is taken as zero. The channel walls are conditioned to be adiabatic. The forced convection heat transfer is carried out inside the channel for different volume fractions and Reynolds numbers. Prandtl number is assumed and fixed as 6.2 same as Abu-Nada [11]. The simulation was carried out to get the isotherm contours and shown for different cases in fig 4. The isotherm is denser at the stagnation wall and symmetry to the cylinder. It gets widened in downstream and spreads along with the cylinder. At the face of the cylinder, the isotherm becomes asymmetrical when the Reynolds number gets increased, figs. 4(b) and 4(c). The temperature is increased when the nanoparticles are introduced in the base fluid 4(d). The stagnation at the front wall makes the conduction dominant due to the velocity becoming zero. The isotherm density is lesser near the rear face when compared to the front face of the cylinder. The convection of the heat transfer is increased when the Reynolds number of the nanofluid is increased gradually. The isotherm is also shown as the cooling effect in 4(e) and 4(f). It is observed that the change in volume fraction is insignificant for isotherm 4(g) and 4(h).

 https://doi.org/10.37896/pd91.3/91342

ISSN: 0369-8963

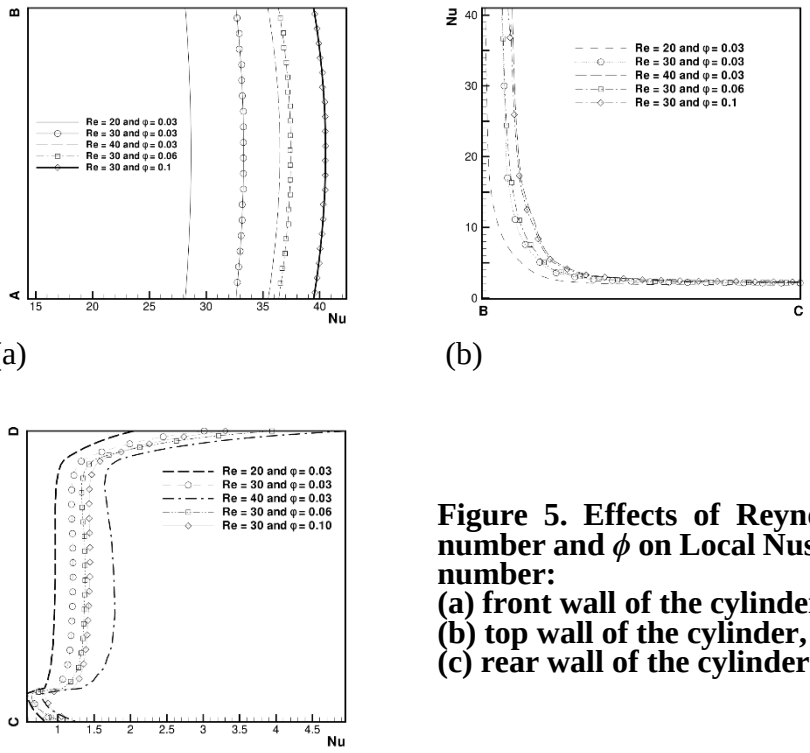

Figure 5. Effects of Reynolds number and ϕ on Local Nusselt number:
(a) front wall of the cylinder,
(b) top wall of the cylinder,
(c) rear wall of the cylinder.

Local and average Nusselt number and their distribution along the cylinder are the important parameters of the current investigation. Due to brevity, the top wall results are represented in this section because the top and bottom walls of the cylinder are showing symmetrical value in Nusselt number distribution 5(b). Fig 5(a) shows the Nusselt number distribution near the front wall (AB). The local Nusselt number is maximum at the stagnation wall when compared to any other wall. The Nusselt number value is higher and decreases along with the corners of the walls than any other place at symmetry plane. A noticeable hike in the Nusselt number is observed when the Reynolds number value is increased from 10 to 20 and the trend continues for the remaining values. The local Nusselt number is increased significantly for the nanofluids than the base fluid. The volume fraction ϕ is varied from 0.03 to 0.1 for the fixed Reynolds number, Re = 30, to understand the significance the volume fraction of nanoparticles. The results clearly show that the conductivity of the nanomaterial improves heat transfer. The local Nusselt number curve is shown in fig 5(b). For this investigation, the considered Reynolds number and ϕ are influencing the local Nusselt number lesser in the downstream. But at the rear wall, the local Nusselt number is more sensitive to both ϕ and Reynolds number fig 5(c). The Nusselt number recorded near the rear wall is lower due to the formation of vortices. But both ϕ and Reynolds number are enhancing the local Nusselt number along the rear wall. Table 2 shows the consolidated average Nusselt number of the cylinder walls. The recorded data clearly shows that nanoparticles are enhancing the heat transfer rate approximately by 11-13% in the average Nusselt number in all walls than the base fluid.

https://doi.org/10.37896/pd91.3/91342

ISSN: 0369-8963

Table 2. Average Nusselt number from the front, top and rear walls of the cylinder (Nu)

Re	ϕ	Front wall average Nu	Top wall average Nu	Rear wall average Nu
10	0.00	16.82	3.09	0.81
20	0.00	25.30	4.21	0.90
30	0.00	29.58	5.17	1.12
40	0.00	32.55	6.03	1.56
20	0.03	28.50	4.41	0.97
30	0.03	34.46	5.23	1.22
40	0.03	36.14	6.35	1.75
30	0.06	37.09	5.3	1.38
30	0.10	40.16	5.92	1.45

Conclusions

The flow over a square cylinder placed in a confined channel was simulated with 2D laminar steady flow. The nanofluid was used to study the forced convection heat transfer inside the channel. The Reynolds number was tested for the laminar range to understand the influence of viscous and inertial forces. The results were produced for both heat transfer and hydrodynamic to understand the role of volume fraction, ϕ. The current results of the study are limited to spherical shaped Ag nanoparticles. Following conclusions were arrived at based on the study.

- At the rear face of the cylinder a pair of wall-attached vortices were formed. The eddy size increases with the increase in Reynolds number. The trend is similar for the volume fraction of the nanoparticles in the base fluid but the Reynolds number is more pronounced in flow separation than the ϕ value.
- Near the cylinder corner the result of friction coefficient value is larger and it decreased in the downstream. The friction coefficient results curve shows a nonlinear tendency for the rear wall for the change in Reynolds number. But the drag coefficient shows the proportionated results. Both the above trends are same for the change in volume fraction.
- At the stagnation face the isotherm is denser than any other faces. The volume fraction is less influenced by the isotherm.
- The local Nusselt number is increased higher than the base fluid when the nanoparticles are introduced in it.
- The front face of the cylinder results in a higher Reynolds number than any other walls due to the stagnation. Along the top wall, the differences in local Nusselt numbers are mainly depending on Reynolds number and ϕ. Nusselt number of the rear wall depends on both Reynolds number and ϕ. The rear wall Nusselt number is lower than all other walls, because of the presence of pair of vortices.

 https://doi.org/10.37896/pd91.3/91342

ISSN: 0369-8963

Nomenclature

C_p	specific heat =J/kgK
H	height of the channel, m
k	thermal conductivity =W/mK
Pr	Prandtl number =ν_f/α_f
Re	Reynolds number =$\overline{u}_o H/\nu$
$\overline{t}$	dimensional time, s
t	nondimensional time
$\overline{u}, \overline{v}$	dimensional velocity components along x, y axes,m/s
u, v	dimensionless velocity components along x, y axes
$\overline{u}_o$	average horizontal velocity at the orifice, m/s
$\overline{x}, \overline{y}$	dimensional Cartesian co-ordinates, m
x, y	dimensionless Cartesian co-ordinates
X_{r1}	dimensionless reattachment length on the bottom wall
X_{r2}	dimensionless reattachment length on the top wall
L	non-dimensional length of the computational domain
H	height of computational domain
T_α	free stream temperature
T_w	surface temperature of the square cylinder
d	width of the square cylinder
X_L	distance between the inlet plane and the front surface of the cylinder

Greek symbols

∞	ambient condition
α	thermal diffusivity,m^2/s
ε	convergence criteria
μ	dynamic viscosity, kg/m-s
ν	kinematic viscosity, m^2/s
ω	dimensionless vorticity
ϕ	volume fraction of the nanofluids
ψ	dimensionless stream function
ρ_f	density of the fluid kg/m^3
ρ_s	density of solid nanoparticles, kg/m^3
θ	no dimensional temperature, $= \frac{T-}{T_w - T_\infty}$
τ_w	all shear stress =$\mu\ \partial u/\partial y$, N/m^2

Subscripts

avg	average
f	fluid
nf	nanofluid
s	solid
w	wall

https://doi.org/10.37896/pd91.3/91342

ISSN: 0369-8963

References

[1] Okajima, A., Strouhal Numbers Of Rectangular Cylinders, J. Fluid Mech., 123 (1982), pp. 379-398
[2] Mukhopadhyay, A., et al., Numerical Investigation Of Confined Wakes Behind A Square Cylinder In A Channel, Int. J. Numer. Methods Fluids, 14 (1992), 12, pp. 1473-1484
[3] Dutta, S., et al., Experimental Investigation Of Flow Past A Square Cylinder At An Angle Of Incidence, J. Eng. Mech., 134 (2008), 9, pp. 788-803
[4] Shankar, A., et al., Numerical Simulation Of Unsteady Low-Reynolds Number Flow Around Rectangular Cylinders At Incidence, J. Wind Eng. Ind. Aerodyn., 69-71 (1997), pp. 189-201
[5] Yoon, D.H., et al., Flow Past A Square Cylinder With An Angle Of Incidence, Phys. Fluids, 22 (2010), 4, pp. 1-12
[6] Sharma, A., Eswaran, V., Heat And Fluid Flow Across A Square Cylinder In The Two-Dimensional Laminar Flow Regime, Numer. Heat Transf. Part A Appl., 45 (2004), 3, pp. 247-269
[7] Mohammed, H.A., et al., Convective heat transfer and fluid flow study over a step using nanofluids: A review
[8] Kakaç, S., Pramuanjaroenkij, A., Review Of Convective Heat Transfer Enhancement With Nanofluids, Int. J. Heat Mass Transf., 52 (2009), 13-14, pp. 3187-3196
[9] Awais, M., et al., Heat Transfer And Pressure Drop Performance Of Nanofluid: A State-Of-The-Art Review, Int. J. Thermofluids, 9 (2021), pp. 100065
[10] Muneeshwaran, M., et al., Role Of Hybrid-Nanofluid In Heat Transfer Enhancement – A Review, Int. Commun. Heat Mass Transf., 125 (2021), pp. 105341
[11] Abu-Nada, E., Application Of Nanofluids For Heat Transfer Enhancement Of Separated Flows Encountered In A Backward Facing Step, Int. J. Heat Fluid Flow, 29 (2008), 1, pp. 242-249
[12] Al-aswadi, A.A., et al., Laminar Forced Convection Flow Over A Backward Facing Step Using Nanofluids, *Int. Commun. Heat Mass Transf., 37* (2010), 8, pp. 950-957
[13] Mohammed, H.A., et al., Influence Of Nanofluids On Mixed Convective Heat Transfer Over A Horizontal Backward-Facing Step, *Heat Transf. - Asian Res., 40* (2011), 4, pp. 287-307
[14] Chandrasekar, M., Suresh, S., A Review On The Mechanisms Of Heat Transport In Nanofluids, *Heat Transf. Eng., 30* (2009), 14, pp. 1136-1150
[15] Hwang, K.S., et al., Flow And Convective Heat Transfer Characteristics Of Water-Based Al2O3 Nanofluids In Fully Developed Laminar Flow Regime, *Int. J. Heat Mass Transf., 52* (2009), 1-2, pp. 193-199
[16] Santra, A.K., et al., Study Of Heat Transfer Due To Laminar Flow Of Copper-Water Nanofluid Through Two Isothermally Heated Parallel Plates, *Int. J. Therm. Sci., 48* (2009), 2, pp. 391-400
[17] Dey, P., Das, A., Analysis Of Fluid Flow And Heat Transfer Characteristics Over A Square Cylinder: Effect Of Corner Radius And Nanofluid Volume Fraction, *Arab. J. Sci. Eng., 42* (2017), 5, pp. 1687-1698
[18] Hojjat, M., Numerical Simulation And Multi-Objective Optimization Of Heat Transfer Of Al2O3/Water Nanofluid In Rectangular Ducts, *Int. J. Therm. Sci., 172* (2022), pp. 107343
[19] Derouich, Y., et al., International Journal Of Heat And Mass Transfer Inclination Effects On Heat Transfer By An Oscillating Square Cylinder In Channel Flow, *Int. J. Heat Mass Transf., 125* (2018), pp. 1105-1120
[20] Brinkman, H.C., The Viscosity Of Concentrated Suspensions And Solutions, *J. Chem. Phys., 20* (1952), 4, pp. 571

 https://doi.org/10.37896/pd91.3/91342

ISSN: 0369-8963

[21] Tiwari, R.K., Das, M.K., Heat Transfer Augmentation In A Two-Sided Lid-Driven Differentially Heated Square Cavity Utilizing Nanofluids, *Int. J. Heat Mass Transf.*, *50* (2007), 9-10, pp. 2002-2018
[22] Khanafer, K., et al., Buoyancy-Driven Heat Transfer Enhancement In A Two-Dimensional Enclosure Utilizing Nanofluids, *Int. J. Heat Mass Transf.*, *46* (2003), 19, pp. 3639-3653
[23] Muthamilselvan, M., et al., Heat Transfer Enhancement Of Copper-Water Nanofluids In A Lid-Driven Enclosure, *Commun. Nonlinear Sci. Numer. Simul.*, *15* (2010), 6, pp. 1501-1510
[24] Santosh Christopher, D., et al., Numerical Investigation Of Heat Transfer From A Two-Dimensional Sudden Expansion Flow Using Nanofluids, *Numer. Heat Transf. Part A Appl.*, *61* (2012), 7, pp. 527-546
[25] Athinarayanan, A.S.K., et al., Numerical Investigation of Heat Transfer from Flow over Square Cylinder Placed in a Confined Channel Using Cu-Water Nanofluid, *Therm. Sci.*, *23* (2019), pp. S1367-S1380
[26] Roache, P.J., Fundamentals Of Computational Fluid Dynamics, 1998, pp. 648
[27] Das, M.K., Kanna, P.R., Application Of An ADI Scheme For Steady And Periodic Solutions In A Lid-Driven Cavity Problem, (2008)
[28] Breuer, M., et al., Accurate Computations Of The Laminar Flow Past A Square Cylinder Based On Two Different Methods: Lattice-Boltzmann And Finite-Volume, *Int. J. Heat Fluid Flow*, *21* (2000), 2, pp. 186-196

 https://doi.org/10.37896/pd91.3/91342